Available online at www.sciencedirect.com

SciVerse ScienceDirect

Ceramics International 38 (2012) 2673–2678

CERAMICS INTERNATIONAL

www.elsevier.com/locate/ceramint

Fabrication of transparent SiO_2 glass by pressureless sintering and spark plasma sintering

Jianfeng Zhang, Rong Tu *, Takashi Goto

Institute for Materials Research, Tohoku University, Sendai 980-8577, Japan

Received 5 October 2011; received in revised form 12 November 2011; accepted 13 November 2011
Available online 22 November 2011

Abstract

Transparent SiO_2 bodies were prepared by pressureless sintering (PLS) and spark plasma sintering (SPS). The effects of sintering and annealing temperature on the transmittance of the SiO_2 bodies were investigated. The SiO_2 bodies sintered by SPS and PLS at 1073–1573 K were amorphous. With increasing the sintering temperature to 1673 K, the SiO_2 bodies sintered by PLS were crystallized while those sintered by SPS were still amorphous. The relative density of the SiO_2 bodies sintered by SPS was 98.5% at 1373 K and 100% at 1573 K, whereas that sintered by PLS was 92.6% at 1373 K and 98.9% at 1573 K. The transmittance was 91.0% and 81.5% at a wavelength (λ) of 2 μm for the SiO_2 sintered bodies by SPS and PLS, respectively. In the ultraviolet range, the transmittance of the SiO_2 bodies sintered by SPS at 1573 K was about 40% at λ = 200 nm and increased to 75% after annealing at 1073 K for 1 h, which was about three times of the transmittance of the SiO_2 bodies sintered by PLS (24.8%).

Keywords: Silica; Glass; Spark plasma sintering; UV–vis–NIR spectroscopy; Transmittance

1. Introduction

Transparent SiO_2 glass has many attractive properties, such as a low thermal expansion coefficient, low electrical conductivity, high chemical resistance and high ultra-violet (UV) light transparency. It is widely used for high efficiency lamps, antenna windows, crucibles for melting high-purity silicon, IC photo-mask substrates, lens material for excimer stepper equipment, and white light phosphors [1,2]. Transparent SiO_2 glass has been commonly fabricated by melting at high temperatures from 2273 to 2573 K. Since SiO_2 glass can be melted by an oxygen–hydrogen gas burner, hydroxyl group elements are easily introduced into the SiO_2 glass, thus inducing an increase in optical loss, particularly in middle to near-infrared region [1]. Other techniques, such as sol–gel, vapor phase axial deposition, pressureless sintering (PLS) of floc-casting [3] and slip-casting [1] green body, and laser micro sintering, have also been used to prepare SiO_2 glass at low temperatures [4,5]. However, when a long sintering process and high sintering temperatures was employed for eliminating residual pores and enhancing transparency, crystallization of SiO_2 glass and a loss of transparency was induced [6].

Spark plasma sintering (SPS) has been applied to densify materials in a short sintering time [7–9]. Many kinds of fully dense structural ceramics [10,11], transparent ceramics [12–14], biomaterials [15], metals [16], and intermetallics [17,18] have been fabricated by using SPS. SPS can also be applied to fabricate dense glass and amorphous materials at a low sintering temperature and short sintering time [19,20]. Mayerhofer et al. had consolidated SiO_2 glass using silicic acid powder (particles size < 10 nm) by SPS at 1273 K and annealing at 1173 K for 5 h; however, the transmittance in the UV–vis spectral region was 63% [19].

In this study, a highly transparent SiO_2 body was fabricated by SPS using commercial SiO_2 powder. The effects of sintering and annealing temperatures on the microstructure and optical properties were investigated. The SiO_2 body was also fabricated by PLS for comparison.

2. Experimental details

Commercial amorphous SiO_2 powder (Admatechs Ltd., Japan, particle size < 500 nm) was passed through a sieve with a pore size of 100 μm and was removed into a graphite die

* Corresponding author.
E-mail address: turong@imr.tohoku.ac.jp (R. Tu).

0272-8842/$36.00
doi:10.1016/j.ceramint.2011.11.034

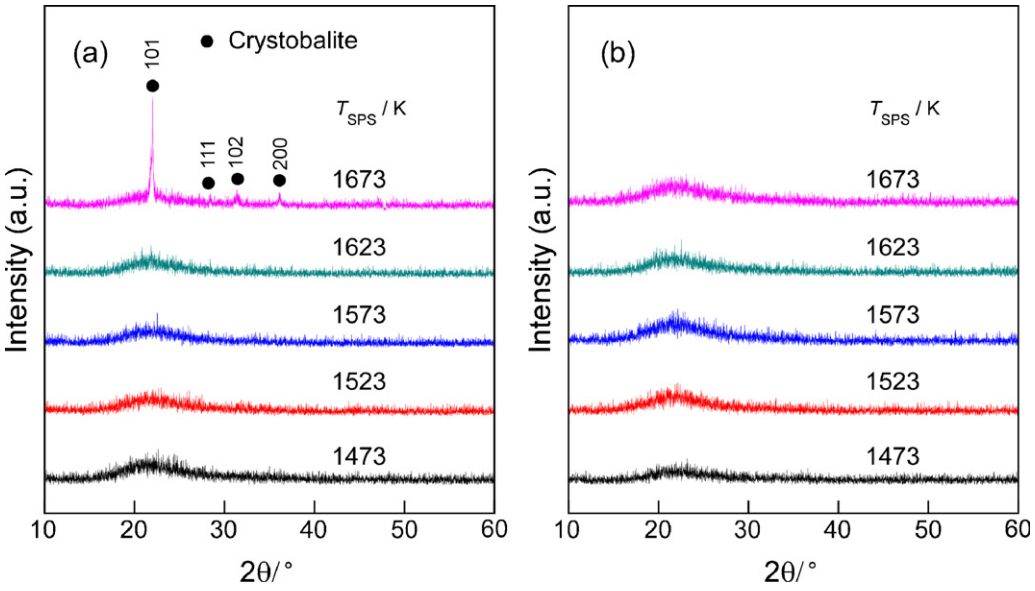

Fig. 1. X-ray diffraction patterns of SiO_2 sintered by (a) PLS and (b) SPS.

(ϕ30 mm × ϕ10 mm × 30 mm). SiO_2 powder was sintered at 1073–1673 K for 10 min with uniaxial pressure of 100 MPa and a heating rate of 100 K min^{-1} by SPS (SPS-210LX, SPS Syntex Inc.). Pulsed direct current (pulses of 60 ms on/10 ms off) was applied. The temperature was measured by an optical pyrometer focused on a hole (ϕ2 mm × 5 mm) in the graphite die. Specimen sintered at 1573 K was annealed at 973–1273 K for 3 h in air. The amorphous SiO_2 powder was also sintered by PLS in air at 1473–1673 K and a heating rate of 0.17 K/s. The specimen was held at the sintering temperature for 7.2 ks, then cooled to room temperature by a rate of 0.17 K/s.

The crystal structure was identified by X-ray diffraction (XRD) with CuKα radiation. The microstructure was observed by scanning electron microscopy (SEM). The bulk density was determined by the Archimedes' method and the relative density was calculated using the theoretical density of SiO_2 (2.2 g cm^{-3}) [21]. Both sides of the SiO_2 body, 1 mm in thickness, were polished for optical measurements. The transmittance in visible and infrared ranges was measured by a spectrophotometer (UV-3101PC, Shimadzu, Japan) in the wavelength (λ) range from 190 to 2500 nm and a Fourier transform infrared spectrometer (FTIR, 460 Plus, Jasco, Japan) in the range from 5000 to 400 cm^{-1} (2–25 μm). A fused silica sample with a thickness of 1 mm was used as a reference. The theoretical transmittance (T_t) of the ultraviolet grade synthetic fused silica [22] was calculated by using Eq. (1) as Ref. [23]

$$T_t = \frac{2n}{n^2+1}, \quad (1)$$

where n is the refraction index of SiO_2.

3. Results and discussion

Fig. 1 shows the X-ray diffraction patterns of SiO_2 sintered by (a) PLS and (b) SPS. Only a broad halo of the SiO_2 bodies sintered by PLS and SPS at 1473–1523 K was detected. At 1673 K, the typical peaks of cristobalite at 2θ of 22.0° (1 0 1), 31.5° (1 0 2) and 36.1° (1 1 1) were detected in the PLS-sintered body, showing crystallization. However, at the same temperature, the SPS-sintered body was amorphous, which implied that SPS was more effective than PLS on depression of SiO_2 crystallization. Yong-Taeg et al. studied the sintering behavior of SiO_2 glasses and reported that vacuum (10^{-4} Pa) was necessary to obtain a SiO_2 body [1]. However, in the present study, no crystallization happened in the SPS process with vacuum of 5 Pa. The reason may be attributed to the rapid temperature increasing rate (100 K min^{-1}) and relatively high pressure (100 MPa) in SPS process.

Fig. 2 shows the effect of sintering temperature on the relative density of SiO_2 bodies sintered by PLS and SPS. The relative density of SiO_2 sintered by PLS increased from 92.5 to

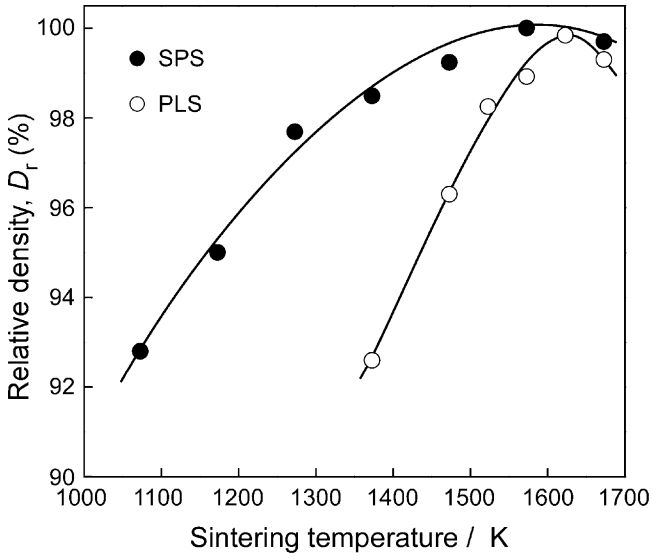

Fig. 2. Effect of sintering temperature on the relative density of SiO_2 bodies sintered by (a) PLS and (b) SPS.

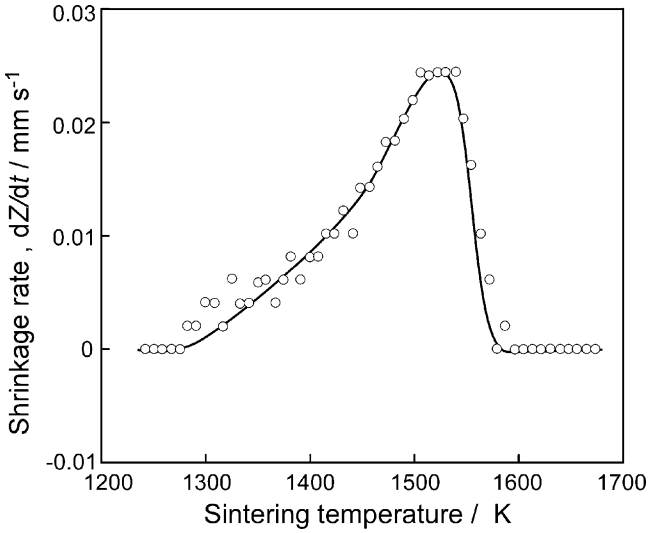

Fig. 3. Effect of sintering temperature on the shrinkage rate of SiO_2 body sintered by SPS.

99.8% with increasing sintering temperature from 1373 to 1623 K, and then slightly decreased to 99.3% at 1673 K. The relative density of SiO_2 sintered by SPS increased from 92.7 to 100% with increasing sintering temperature from 1073 to 1573 K and slightly decreased to 99.7% at 1673 K. Yong-Taeg et al. [1] had sintered SiO_2 powder at 1573–1873 K at a heating rate of 17 K min^{-1} in high vacuum. A fully dense SiO_2 body was obtained by heating for 30 min at 1673 K. The sintering temperature was 100 K higher and the holding time was three times of that applied in the present study (1573 K and 10 min). Fig. 3 shows the effect of sintering temperature on the shrinkage rate of the SiO_2 bodies sintered by SPS. The shrinkage of SiO_2 body started from 1200 K and ended at 1573 K.

Fig. 4 shows the fracture microstructure of the SiO_2 bodies sintered by PLS at 1523–1673 K. SiO_2 grains 0.5–1 μm in diameter were observed at 1523 K, indicating significant necking and grain growth (Fig. 4(a)). At 1573 K, grains were no longer observed, whereas many small pores about 100 nm in diameter were observed (Fig. 4(b)). At 1623 K, dense and glassy microstructure was observed (Fig. 4(c)). At 1673 K, crystallization partially occurred (Fig. 4(d)). Fig. 5 shows the fracture microstructure of the SiO_2 body by SPS at 1173–1673 K. The grain size of the SiO_2 body at 1173 and 1273 K was almost the same as that of raw powder (Fig. 5(a) and (b)). At 1373 K, the maximum SiO_2 grain size was over 2 μm in diameter (Fig. 5(c)). Above 1473 K, the SiO_2 body was fully sintered and no grains were identified. There were small pores in the SiO_2 bodies sintered at both 1473 (Fig. 5(d)) and 1673 K (Fig. 5(f)), but no pores were identified at 1573 K (Fig. 5(e)). This was in accord with the trend of the relative density shown in Fig. 2.

Fig. 6 shows the IR-transmittance spectra of the SiO_2 body sintered by (a) PLS and (b) SPS as a function of wave number (N_w) from 2000 to 5000 cm^{-1}. The peaks at N_w = 2259.2 cm^{-1} represented the second harmonic of the asymmetric Si–O–Si stretching vibration [24], and those at 3761.8 cm^{-1} were attributed to the stretching vibration of SiO–H [19]. At

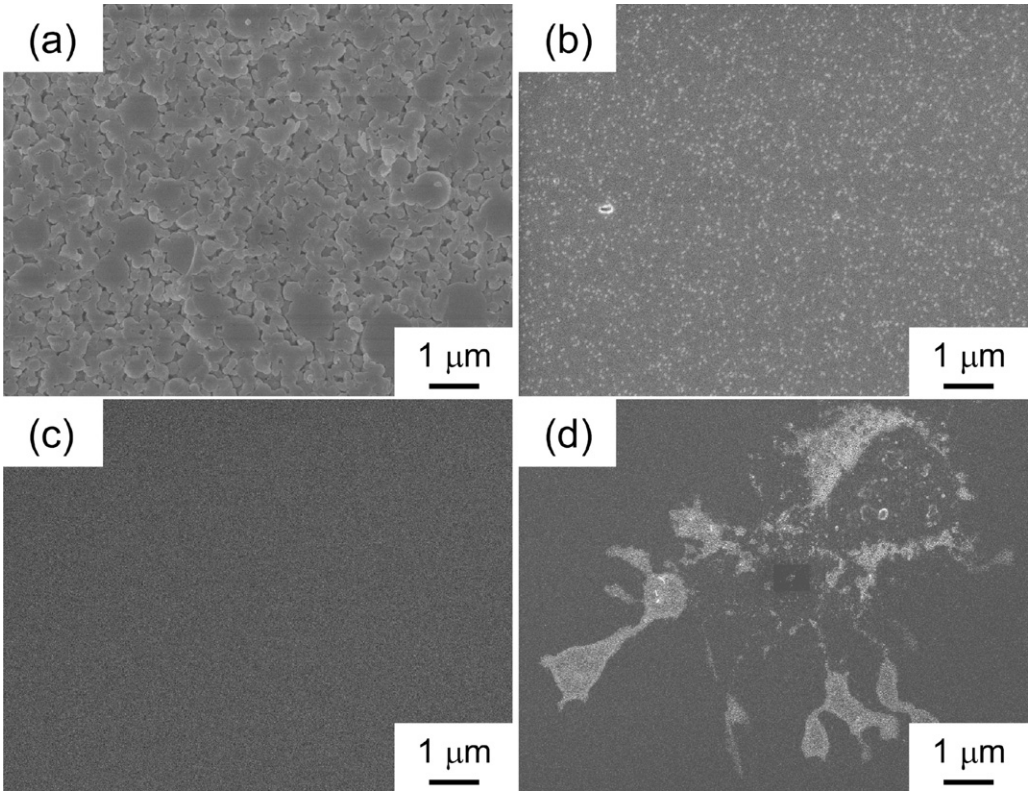

Fig. 4. Fracture surfaces of the SiO_2 bodies sintered by PLS at (a) 1523, (b) 1573, (c) 1623, and (d) 1673 K.

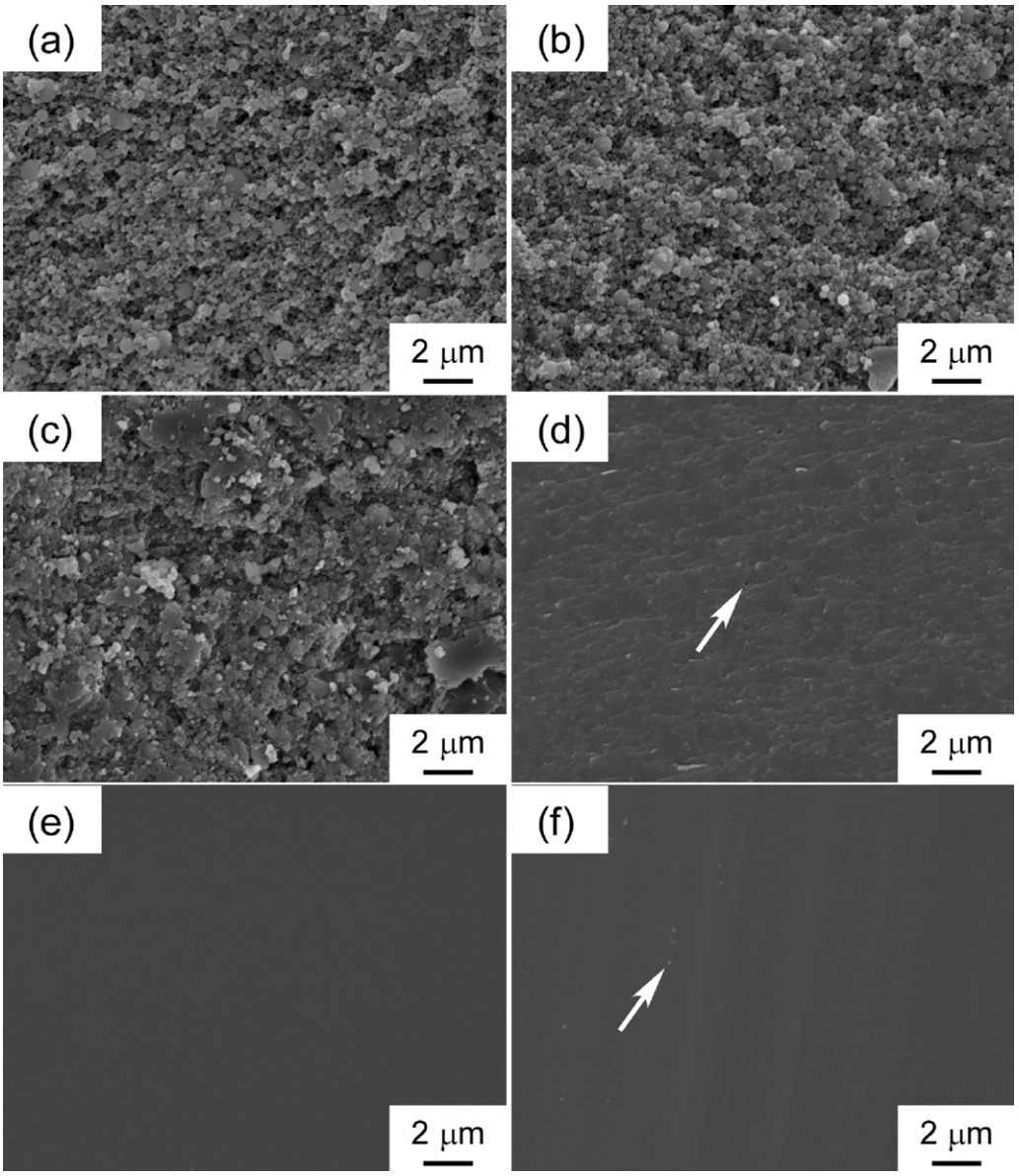

Fig. 5. Fracture surfaces of the SiO_2 bodies sintered by SPS at (a) 1173, (b) 1273, (c) 1373, (d) 1473, (e) 1573, and (f) 1673 K.

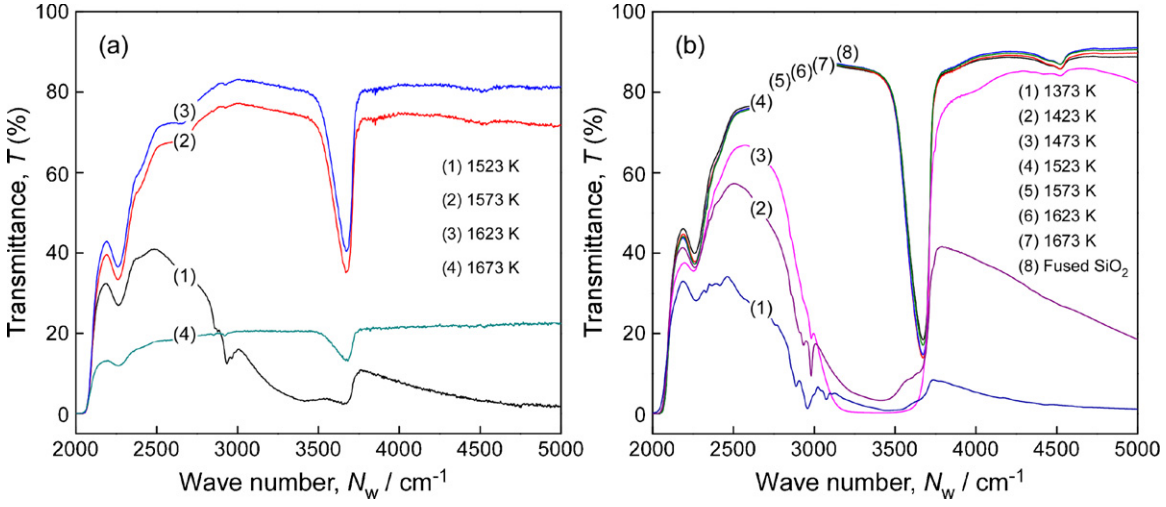

Fig. 6. IR-transmittance spectra of the SiO_2 bodies sintered by (a) PLS and (b) SPS as a function of wave number (N_w) from 2000 to 5000 cm^{-1}.

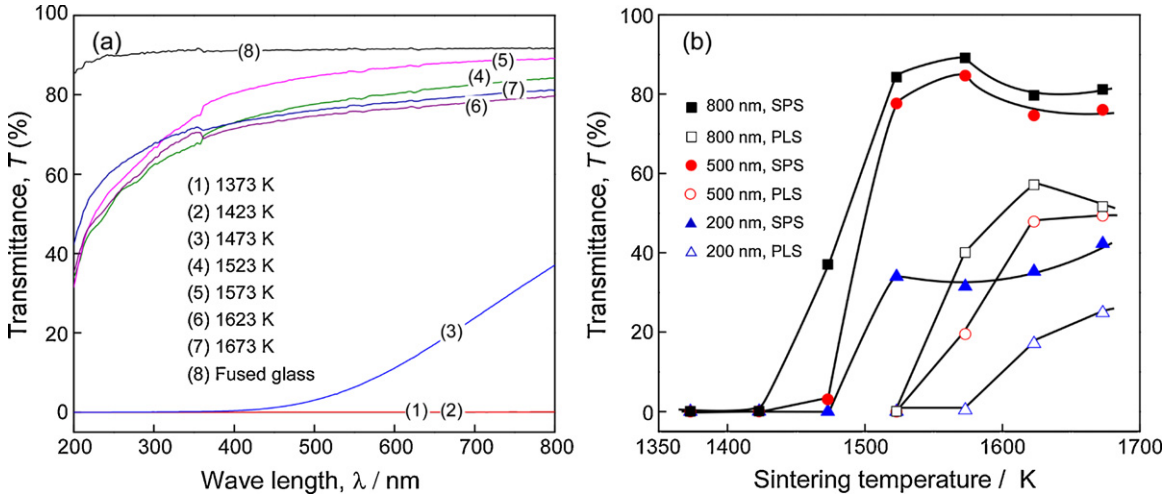

Fig. 7. (a) UV–vis-transmittance of SiO_2 bodies sintered by SPS at different temperatures, (b) UV–vis-transmittance comparison of SiO_2 bodies sintered by PLS and SPS.

$N_w = 5000\ cm^{-1}$, the transmittance of the SiO_2 body (T) sintered by PLS at 1623 K showed the highest value of 81.5%. On the other hand, the transmittance of the SiO_2 body (T) sintered by SPS at 1573 K and $N_w = 5000\ cm^{-1}$ showed the highest value of 91.4%, close to that of the fused SiO_2 (91.5%) and the theoretical value (93.2%).

Fig. 7(a) shows the transmittance (T) of the SiO_2 body by SPS as a function of wave length (λ) in the UV–vis range of 200–800 nm. At the sintering temperatures of 1373 and 1423 K, the SiO_2 body was opaque. At 1473 K, the T increased from 0 to 37% at λ = 400–800 nm. At 1523–1673 K, the T at λ = 200 nm increased from 35% to 45%, almost half that of the fused SiO_2. With increasing λ from 200 to 500 nm, the T increased from 45 to 85%. Fig. 7(b) shows the T of the SiO_2 body sintered by PLS and SPS at 200, 500 and 800 nm as a function of sintering temperature. At 1523 K, the T of the SiO_2 body sintered by PLS was almost 0 at 200 to 800 nm. The maximum T of the SiO_2 body sintered by PLS at 1623 K was 49 and 51% at 500 and 800 nm, respectively. With an increase of sintering temperature from 1473 to 1523 K, the T of the SiO_2 body sintered by SPS increased to 35% at λ = 200 nm and 82% at λ = 800 nm, respectively. The T of the SiO_2 body sintered by SPS at 1573 K showed the maximum value of 89.1% at λ = 800 nm, about 95% that of the theoretical value. At λ = 200 nm, the T of the SiO_2 body sintered by SPS increased from 35 to 45% with an increase in the sintering temperature from 1523 to 1673 K.

Fig. 8(a) shows the T of the SiO_2 bodies sintered by SPS and annealed at various temperatures from 973 to 1173 K. The transmittance reported by Hiratsuka et al. [3] and Mayerhofer et al. [19] was included for comparison. The T at λ = 200–500 nm increased with increasing annealing temperature from 973 to 1073 K and slightly decreased at λ = 800 nm. With increasing annealing temperature to 1173 K, the T decreased independent of λ. Mayerhofer et al. consolidated SiO_2 nanoparticles by SPS at 1273 K and annealed them at 1173 K for 5 h [19]. The as-sintered SiO_2 body showed a T of 63% in the UV–vis range of λ = 200–1000 nm. Using PLS, Hiratsuka et al. fabricated a SiO_2 body of a floc-cast green body in air. The T of the SiO_2 body was 85% at λ = 400–1000 nm, but

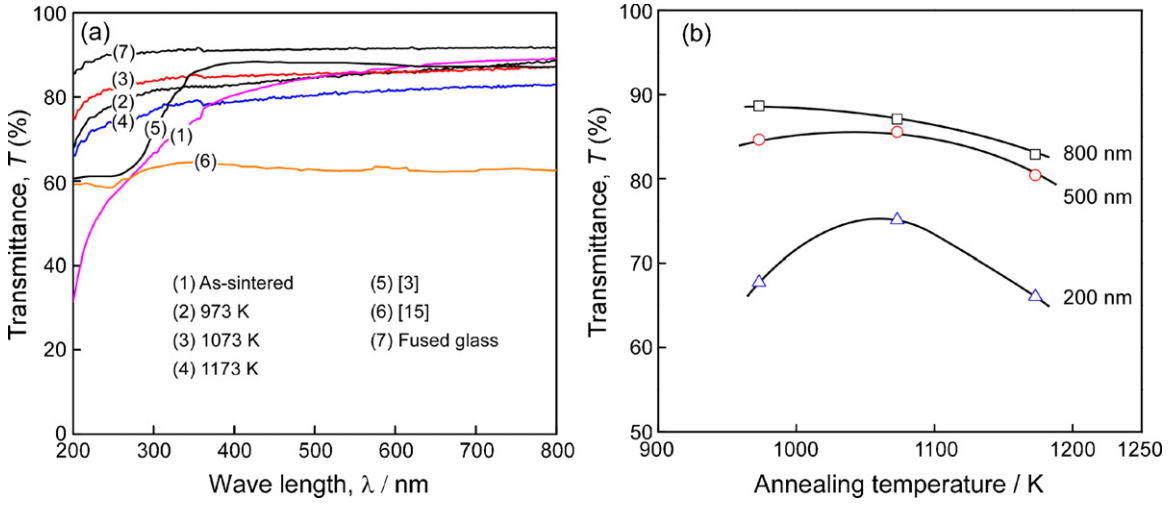

Fig. 8. UV–vis-transmittance spectra of the SiO_2 bodies sintered by SPS as a function of (a) wave length and (b) annealing temperature.

61% at $\lambda = 200$ nm. Fig. 8(b) shows the T of the SiO_2 body sintered by SPS at 1573 K as a function of annealing temperature. At $\lambda = 200$ nm, the SiO_2 body sintered at 1573 K and annealed at 1073 K showed a maximum T of 75%. This value was 20% higher than those reported by Hiratsuka et al. [3] and Mayerhofer et al. [19].

4. Conclusions

Transparent SiO_2 bodies were prepared by PLS and SPS at 1173–1673 K. The relative density of the SiO_2 body sintered by PLS showed the maximum value of 98.9% at 1573 K, whereas that of the SiO_2 body sintered by SPS was 100% at 1573 K. The SiO_2 body sintered by PLS showed partial crystallization at 1623 K whereas no crystallization was observed up to 1673 K in that sintered by SPS.

The transmittance of the SiO_2 body sintered by SPS at 1523–1673 K was above 90% at $\lambda = 2$ μm. The transmittance of the SiO_2 body sintered at 1573 K and annealed at 1073 K had the maximum values of 75 and 87% at $\lambda = 200$ and 800 nm, respectively, almost three times of that of the SiO_2 body sintered by PLS.

Acknowledgements

This research was financially supported by the Japan Society for the Promotion of Science (JSPS), Grant-in-Aid for JSPS fellow 22-00365, the Rare Metal Substitute Materials Development Project, the New Energy and Industry Technology Development Organization (NEDO) and the Global COE Program ''Materials Integration (International Center of Education and Research), Tohoku University.''

References

[1] O. Yong-Taeg, S. Fujino, K. Morinaga, Fabrication of transparent silica glass by powder sintering, Science and Technology of Advanced Materials 3 (2002) 297–301.
[2] T. Uchino, T. Yamada, White light emission from transparent SiO_2 glass prepared from nanometer-sized silica particles, Applied Physics Letters 85 (7) (2004) 1164–1166.
[3] D. Hiratsuka, J. Tatami, T. Wakihara, K. Komeya, T. Meguro, Fabrication of transparent SiO_2 glass from pressureless sintering of floc-cast green body in air, Journal of the Ceramic Society of Japan 115 (6) (2007) 392–394.
[4] A. Streek, P. Regenfub, T. Sub, R. Ebert, H. Exner, Laser micro sintering of SiO_2 with an NIR-laser, Proceedings of SPIE, the International Society for Optical Engineering 6985 (2008), 6985Q.1-8.
[5] N.K. Tolochko, M.K. Arshinov, K.I. Arshinov, A.V. Ragulya, Laser sintering of SiO_2 powder compacts, Powder Metallurgy and Metal Ceramics 43 (1–2) (2004) 10–16.
[6] E.M. Rabinovich, Preparation of glass by sintering, Journal of Materials Science 20 (1985) 4259–4297.
[7] M. Omori, Sintering, consolidation, reaction and crystal growth by the spark plasma system (SPS), Materials Science and Engineering A 287 (2000) 183–188.
[8] R. Orrù, R. Licheri, A.M. Locci, A. Cincotti, G. Cao, Consolidation/synthesis of materials by electric current activated/assisted sintering, Materials Science and Engineering: R: Reports 63 (4–6) (2009) 127–287.
[9] M. Nygren, Z.J. Shen, On the preparation of bio-, nano- and structural ceramics and composites by spark plasma sintering, Solid State Sciences 5 (1) (2003) 125–131.
[10] Z.J. Shen, Z. Zhao, H. Peng, M. Nygren, Formation of tough interlocking microstructures in silicon nitride ceramics by dynamic ripening, Nature 417 (2002) 266–269.
[11] M. Hotta, Densification and phase transformation of b-Sialon-cubic boron nitride composites prepared by spark plasma sintering, Journal of the American Ceramic Society 92 (8) (2009) 1684–1690.
[12] K. Morita, B.N. Kim, H. Yoshida, K. Hiraga, Spark-plasma-sintering condition optimization for producing transparent $MgAl_2O_4$ spinel polycrystal, Journal of the American Ceramic Society 92 (6) (2009) 1208–1216.
[13] R. Chaim, Z. Shen, M. Nygren, Transparent nanocrystalline MgO by rapid and low-temperature spark plasma sintering, Journal of Materials Research 19 (2004) 2527–2531.
[14] R. Chaim, R. Marder-Jeackel, Z. Shen, Transparent YAG ceramics by surface softening of nanoparticles in spark plasma sintering, Materials Science and Engineering A 429 (2006) 74–78.
[15] Z.J. Shen, E. Adolfsson, M. Nygren, L. Gao, H. Kawaoka, K. Niihara, Dense hydroxyapatite–zirconia ceramic composites with high strength for biological applications, Advanced Materials 13 (3) (2001) 214–216.
[16] S.W. Wang, L.D. Chen, Y.S. Kang, M. Niino, T. Hirai, Effect of plasma activated sintering (PAS) parameters on densification of copper powder, Materials Research Bulletin 35 (2000) 619–628.
[17] Q. He, C.C. Jia, J. Meng, Influence of iron powder particle size on the microstructure and properties of Fe_3Al intermetallics prepared by mechanical alloying and spark plasma sintering, Materials Science and Engineering A 428 (1–2) (2006) 314–318.
[18] T. Skiba, P. Haušild, M. Karlik, K. Vanmeensel, J. Vleugels, Mechanical properties of spark plasma sintered FeAl intermetallics, Intermetallics 18 (7) (2010) 1410–1414.
[19] T.G. Mayerhofer, Z. Shen, E. Leonova, M. Eden, A. Kriltz, J. Popp, Consolidated silica glass from nanoparticles, Journal of Solid State Chemistry 181 (2008) 2442–2447.
[20] L.J. Wang, W. Jiang, L.D. Chen, Z.J. Shen, Formation of a unique glass by spark plasma sintering of a zeolite, Journal of Materials Research 24 (10) (2009) 3241–3245.
[21] JCPDS, International Centre for Diffraction Data, No. 27-0605.
[22] http://www.sciner.com/Opticsland/FS.htm.
[23] C. Wang, Z. Zhao, Transparent $MgAl_2O_4$ ceramic produced by spark plasma sintering, Scripta Materialia 61 (2009) 193–196.
[24] A.M. Boies, J.T. Roberts, S.L. Girshick, B. Zhang, T. Nakamura, A. Mochizuki, SiO_2 coating of silver nanoparticles by photoinduced chemical vapor deposition, Nanotechnology 20 (2009) 1–8, 295604.